The Upper Atmosphere Composition Spectrometer

D. C. Kayser,* W. T. Chater,† C. K. Howey,† and J. B. Pranke*
The Aerospace Corporation, Los Angeles, California

The Upper Atmosphere Composition Spectrometer (UACS) was flown on the Department of Defense Space Test Program mission S85-1. This paper describes the instrument and discusses examples of its operation in orbit. UACS employs a conventional quadrupole mass filter with a semi-open ionization chamber and a special dual detector system for a large dynamic measurement range. In addition to measuring neutral gas composition for masses 4 to 48, UACS performs a retarding potential analysis of the incident neutral gas stream to measure atmospheric temperature and one component of the neutral wind. Major features of the instrument design were validated. In particular, both the dual detector and the retarding potential energy analysis (RPA) systems worked well.

Nomenclature

E = gas particle kinetic energy in satellite reference frame
f = distribution function of v or E
F = density-enhancement factor
k = Boltzmann's constant
m = mass of a gas specie
N_a = ambient number density
N_s = ion source number density
S = ratio of gas particle velocity to thermal velocity
T_a = ambient neutral gas temperature
T_s = ion source gas temperature
v = ambient gas thermal velocity
V = satellite velocity
θ = half-angle of the chamber orifice
ϕ = gas ram angle measured from entrance normal

Introduction

IN the last two decades, satellite-borne neutral composition experiments have contributed substantially to our understanding of the dynamics and chemistry of the Earth's upper atmosphere. Futhermore, in conjunction with charged particle and remote sensing measurements, they have provided the detailed observations needed to improve our understanding of the basic physics of auroral and solar heat inputs, as well as satisfying more immediate needs for improved empirical models of composition. Over time, composition measurement techniques have been modified and improved, giving in recent years greater measurement accuracy and versatility. Presently, with the exception of atomic hydrogen, routine density measurements of all significant thermospheric species can be made at altitudes between 130 and 1000 km.

Techniques for the measurement of neutral wind and temperature were developed later, and are still being refined. In consequence, the present data base for the neutral upper atmosphere is extensive but uneven with regard to measurement accuracy and completeness. Most recently, Hedin[1] discussed the need for additional coverage at high latitudes during high solar activity, as well as coverage at low altitudes generally. In addition, disagreements between in situ and remotely sensed temperature data suggest the need for further measurements. It is thus desirable that measurements of the neutral thermosphere be continued for the foreseeable future, preferably into the period of next solar maximum (~1992).

The Upper Atmosphere Composition Spectrometer (UACS) was designed to operate on satellites that are flown in the mid and lower thermosphere. The instrument makes routine measurements of He, O, N_2, Ar, and O_2 composition and allows further testing of some unconventional measurement techniques. It will be seen that even though UACS employs an electrostatic quadrupole mass filter in the style of the closed-source sensor described by Peltz et al.,[2] its overall concept resembles the one used in the so-called quasi-open source mass spectrometer of Nier et al.[3] Atomic and molecular oxygen separation follows techniques described in Nier et al.[4] and Kayser and Potter.[5] The "fly-through" analysis of Nier et al.[4] has been extended to allow a full retarding potential energy analysis (RPA) of the incident gas stream, thereby affording another technique for measurement of neutral temperature and wind. Neutral RPA without mass analysis was demonstrated early on by Philbrick et al.[6] RPA combined with mass analysis complements the baffle method of Spencer et al.[7,8] and was described as a feature of the Dynamics Explorer Wind and Temperature Spectrometer.[8] However, to date no results have been published which demonstrate that a swept RPA has been successfully applied to neutral composition measurements.

UACS was recently flown on Department of Defense Space Test Program mission S85-1. The mission was flown in a polar, nearly circular orbit at approximately 200 km altitude, thus providing a suitable environment for evaluation of the design. While this paper is intended primarily to describe the instrument, we are also able to show preliminary flight data which illustrate its major operational features.

Technique

The technique used for satellite-based mass spectrometer measurements of composition relies on two underlying relationships: The first prescribes the ion source number density, N_s, of each gas species as a function of ambient density, N_a. For example, following the derivation of Hedin et al.,[9] when the ion source region consists of a spherical thermalizing chamber, N_s is given by

$$N_s = N_a\{\sqrt{T_a/T_s}\,F(S)\cos^2(\theta/2)+1\} \tag{1}$$

where

$$F(S) = \exp(-S^2)+\pi^{1/2}S[1+\mathrm{erf}(S)] \tag{2}$$

and

$$S = [m/(2kT_a)]^{1/2}V\cos\phi \tag{3}$$

Here T_a and T_s are, respectively, the ambient and source temperatures, θ is the half-angle of the chamber orifice as measured from entrance normal, m is the species mass, k is

Received June 10, 1985; revision received Oct. 8, 1985.

*Member Technical Staff, Space Sciences Laboratory.
†Senior Engineer, Space Sciences Laboratory.

Boltzmann's constant, V is the satellite velocity (plus any wind component in the ram direction) and ϕ is the gas ram angle measured from entrance normal. Consideration of Eq. (1) for $V = 8000$ m/s and small ram angles shows that N_s is essentially independent of T_a. For UACS, the $F(S)$ term of Eq. (1) requires modification to account for a more complex source geometry.

A second relationship is required to specify the proportionality between the instrument detector output and the ionizing chamber gas density. Because this proportionality depends on numerous design details, it is determined by calibration. Combined, the two relationships allow a determination of ambient density from instantaneous detector output in a manner that is insensitive to ambient wind and temperature. These latter quantities must be determined separately. One method of wind and temperature measurement[7] modulates the incident gas flow with an external mechanical baffle, and the resulting signal variation is analyzed to yield temperature and crosswind components. The ram component of the wind must be obtained by yet another method, as detailed below.

Evaluation of Eq. (1) with typical parameter values shows that gas density in the thermalization chamber is largely determined by the term involving $F(S)$, which represents the contribution of the thermalized out-flowing gas component, while the contribution of the streaming inflowing gas (term 2) is small. For example, at satellite velocities, the ratio of terms is 60:1 or more for N_2. Conventional mass spectrometer operation cannot distingush between these components and thus produces a sum of signals nearly proportional to the larger thermalized gas density. However, when a streaming particle is ionized by electron bombardment, it retains the signature of the ambient gas, namely velocity and direction imparted by bulk motion of the gas, V, plus a thermal velocity, v, representative of the ambient thermal distribution function, $f(v,m)dv$. With a velocity of 8 km/s in the satellite reference frame, the ion will have a typical energy of .33 eV/AMU, compared with .005 eV/AMU or less for an ion derived from the thermalized gas of the ion source. A 2-V potential barrier at the ion source exit will, as a consequence, pass streaming ions of O, N_2, and O_2 (5.3, 9.2, and 10.6 V typical) while repelling thermal ions. Composition, temperature, and large crosswinds (on spun satellites) have been successfully measured with mass spectrometers modified in this manner.[4,10,11]

Sweeping the potential barrier to achieve a full retarding potential analysis of the streaming gas energy distribution, and hence temperature and wind, is a logical extension of the barrier technique. Figure 1 is a plot of typical particle energy distributions $f(E,m)$ obtained when $f(v,m)$ is transformed into the satellite reference frame. Because the energy analysis is done with a flat grid, $f(E,m)$ describes only the ram component of energy. No information on crosswind components is obtained from this method. It should be noted that the species distributions overlap extensively, implying that an energy analysis without mass separation would be ambiguous. A wind component, dV, in the ram direction will shift the distributions in energy by the fraction $dE/E \approx 2dV/V$. As an example, a 100 m/s wind will shift the N_2 distribution maximum from 9.3 to 9.53 V, an easily detected change. Distribution width is a measure of the ambient gas temperature.

The signal obtained from the RPA analysis is in the form of a cumulative distribution curve; that is, the signal represents the population of all particles with energies greater than the instantaneous barrier voltage. Figure 2 shows three such curves, corresponding to $T_a = 1000$ K, and winds of +200, 0, and −200 m/s in the ram direction. For simplicity, the calculation assumes no energy discrimination after the RPA grid. The change in curve shape with temperature is illustrated in Fig. 3. These distributions correspond to typical extremes (700-1500 K) encountered in daytime measurements above 200 km altitude.

The wind component can be obtained directly from shifts in the position of the RPA curve, after accounting for the satellite velocity. Based on the above graphical illustration, accuracies of 50 m/s or better should be obtainable without elaborate processing. Extraction of temperatures accurate to 50 K or better may require refined numerical techniques which account for instrumental transfer characteristics and the resultant curve distortion. In a later section of the present work we include an example of an RPA curve obtained by UACS on S85-1. These preliminary data are consistent with design expectations.

Previous measurement programs have shown the utility of conventional mass spectrometer measurements in the determination of He, N_2, Ar, and atomic oxygen (above 220 km) composition. Additionally, with ion sources of special construction, atomic oxygen and O_2 concentrations can be ob-

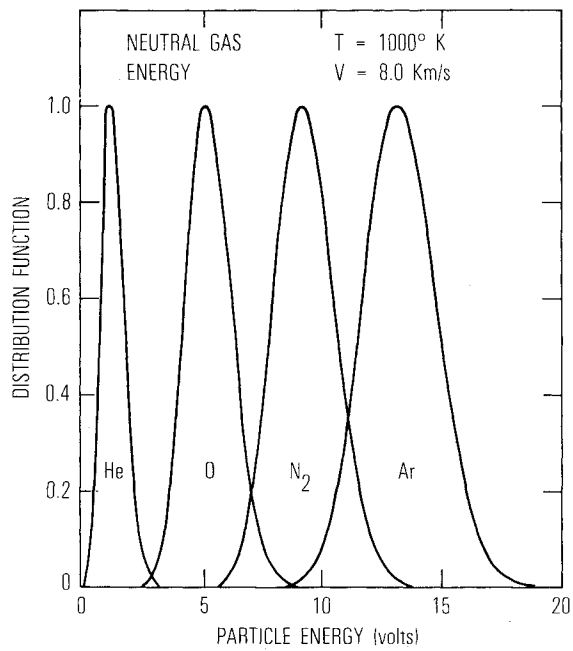

Fig. 1 Neutral particle energy distributions in the satellite reference frame for typical gases.

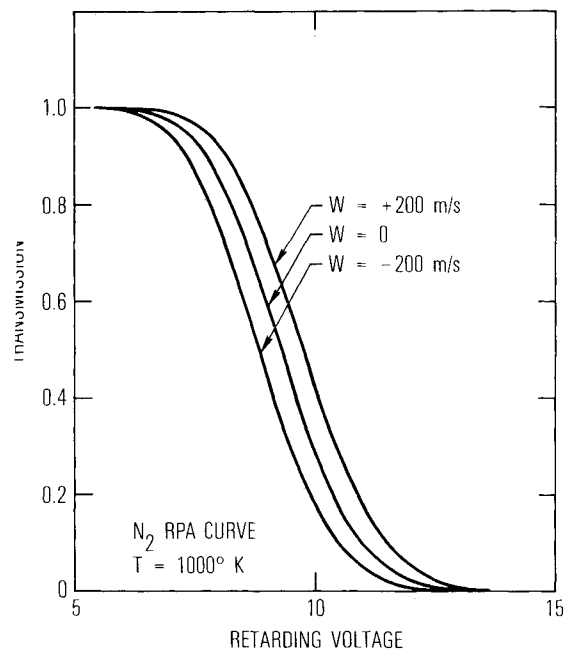

Fig. 2 Calculated retarding potential transmission curves show the displacement effect of winds.

tained at all satellite altitudes.[5] The UACS was designed to exploit previous techniques, thereby providing the capability to measure complete composition in the lower thermosphere along with neutral temperature and the ram wind component. The instrument flown reflects the multiplicity of requirements and constraints of the different measurement techniques, and departs from previous experiments more in specific details than in overall design. The remainder of this section discusses briefly some of the most important design considerations.

Angular sensitivity: At satellite velocities, the streaming gas component is sharply peaked about ram with an e-folding width less than 10 deg.[4] A sensor with high angular sensitivity would detect small departures in orientation from ram, or equivalently, crosswind perturbations of the gas stream, as seemingly random signal variations. The quadrupole mass filter and custom-designed ion lens allow wide-angle focus, thereby minimizing this problem, while providing sufficient resolution (1-1.5 AMU) and high sensitivity.

Ion source geometry: The region where ionization occurs must view the ambient through a cone of half-angle ~ 15 deg or more to fully sample the incident gas distribution. Otherwise, the RPA mode sensor output will be a function of ambient temperature. Additionally, the open geometry is necessary to illuminate the ionization chamber for the O and O_2 separation technique of Ref. 5, and has a side benefit of reducing the source background pressure. The RPA technique requires that the ionizing region, ion lens, and quadrupole be in line with the gas stream.

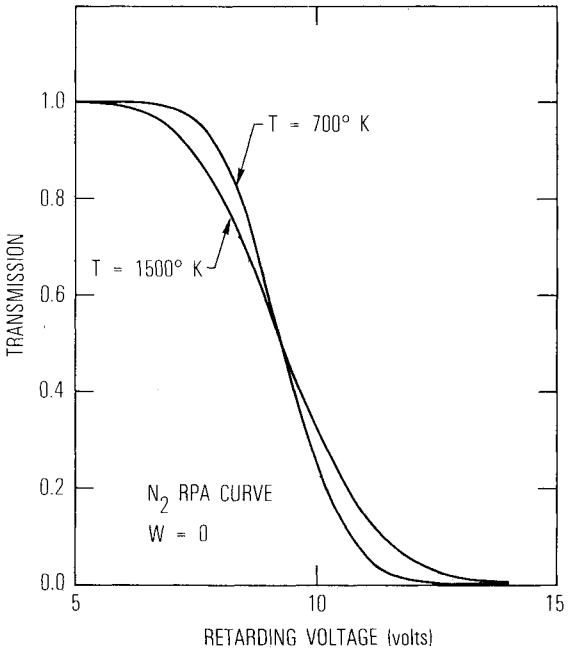

Fig. 3 Calculated retarding potential transmission curves show curve shape variation with temperature.

Dynamic range: Composition measurements in the thermosphere require nearly simultaneous detection of minor species with densities of $10^6/cm^3$ or less along with major species at $10^{10}/cm^3$ or more. Also, retarding potential analysis produces inherently weak signals because it operates only on the streaming gas component. Single-detector systems must compromise between detector noise limitations on the low-signal end and overload on the high-signal end. Schemes involving series detectors of different sensitivities solve the dynamic range problem but must deal with overload and possible damage to the high-sensitivity detector when high-intensity peaks are selected. The UACS design places the high-sensitivity detector (abbreviated in this paper as SID, for Spiraltron ion detector) at right angles to the quadrupole axis and employs an electrostatic deflector to steer the beam for detection of low-intensity peaks.

Instrumentation

A cross-sectional view of the UACS sensor in its vacuum housing is given in Fig. 4. The source vacuum cover and cutter mechanism (A) have been described previously.[3] Sealed at calibration, the sensor remains evacuated until operations in orbit are begun. At that time, a cutter-wheel mechanism is activated, which severs the outer vacuum can. The cutter assembly and vacuum cap deploy on a pivot arm (not shown) to an aft stored position. The source entrance collimator (B) remains to define gas flow conditions into and out of the sensor. Gas enters the ion source (C), to be ionized by a crossed electron beam from one of two redundant electron guns (D).

Ions so produced are extracted and focused by an electrostatic lens (E) into the quadrupole mass filter (F). Ions of the selected mass exit the filter into a Faraday cup (G). The cup has a small exit hole to pass a few percent of the ions. When the electrostatic deflector (H) is enabled, these ions are sent to the entrance cone of a Spiraltron electron multiplier (I). The cone is held at −3200 V behind two high-transmission shield grids in the deflector assembly.

The sensor was designed to be entirely bakeable to minimize residual contamination and promote stability of electrically critical surfaces. The vacuum housing and many internal parts are of stainless steel. Electrical isolation is provided by machined ceramic stand-offs, brazed assemblies, and glass feedthroughs. Vacuum flanges are gasketed with gold rings. The Spiraltron electron multiplier (model #4219 EIL from Galileo Electro-Optics Corporation) is bakeable. Before calibration, the calibration chamber and the mated sensor are baked at temperatures in excess of 170°C. After calibration, the source vacuum cap is sealed in place without breaking the vacuum. An integral Vac-Ion pump maintains high-quality vacuum in the period between the end of calibration and launch. The pump is flown without a magnet and is not operated in orbit. Electronics and sensor are packaged together for a total weight of 9 kg.

Fig. 5 is an electrical block diagram of UACS. The instrument receives from the spacecraft 28-V unregulated power, commands, a frequency reference, telemetry control signals,

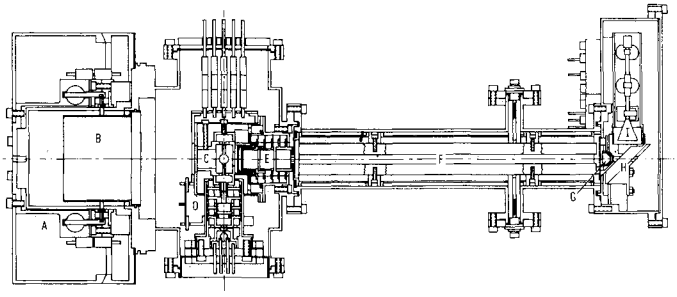

Fig. 4 UACS sensor including vacuum housing.

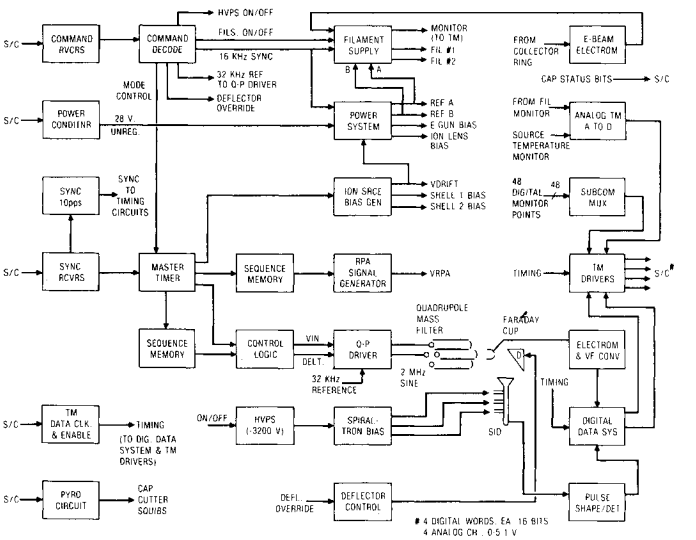

Fig. 5 UACS electronics block diagram.

and pyrotechnic firing current. The instrument returns serial digital data at 640 b/s, along with two cap-cutter status bits, and four analog housekeeping voltages. Instrument state is imposed by signals on the lines HVPS (high-voltage power supply) on/off, filaments on/off, deflector override, and mode control. Either of two filaments may be on, and there are five mass program modes, corresponding to a spectrum scan from 4 to 48 mass units, a scan from 4 to 48 mass units with the RPA grid set at +2 V, a mode to energy analyze N_2, another to energy analyze N_2 plus sample composition at five other masses, and a mode to energy analyze, in turn, O, N_2, and O_2. Not all possible configurations lead to useful instrument states; the most useful combinations have been recoded into a set of 32 commands. Operating power is 8 W, divided among electronics (2 W), filament (3 W), and quadrupole driver (3 W).

The UACS instrument incorporates a number of design features which are intended to provide the high degree of stability necessary for absolute measurements of composition. Past source designs have typically positioned the filaments close to the ionizing region, thereby insuring a stable electron current, but with a concomitant intense heat source that produces thermal transients at turn-on. UACS uses an electrostatic lens (D in Fig. 4) to provide a parallel beam of electrons at the point of ionization, allowing the filament to be positioned 3.8 cm away. Heat generated by the filament is conducted into the vacuum flange and sensor body, and the ionization chamber is heat-sunk to the ceramic spacer assembly. As a result, the ionization chamber temperature changes by only a few degrees after filament turn-on. Source temperature is monitored through a linear, calibrated temperature sensor.

With a remotely spaced filament, some penalty is incurred through increased susceptibility of the electron beam to magnetic fields. To compensate, the electron beam is regulated closed loop at 50 ($\pm$0.1) μa, using the current collected on the source collector ring (shown in Fig. 6). This scheme insures that a 50-μa current crosses the chamber at the point of ionization, whereas regulation on filament emission current would not compensate for any beam deflection or transmission losses.

Figure 6 shows some detail of the ionizing chamber. Neutrals (n) enter at the left, are ionized (n+) by a crossed electron beam (e), and are focused at the right (see Fig. 4) into the quadrupole (Q-P). For the normal mode, shells 1 and 2 are biased so that the +10 V potential line is along the electron beam path and ions are accelerated toward the ion lens. For the RPA mode, shell 1 bias is set equal to the shell 2 bias, creating a drift space, and the retarding electrode voltage is swept to effect the energy analysis.

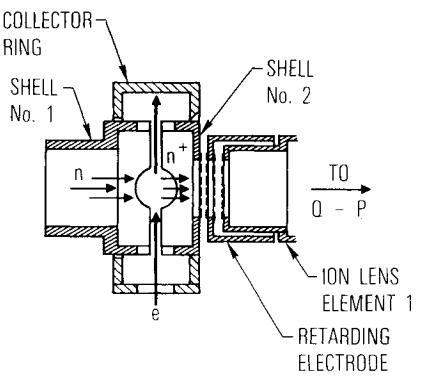

Fig. 6 Detail of the ionizing chamber.

The electric field configuration of the ion lens (E, in Fig. 4) was selected to provide focusing for both thermalized and streaming ions, depending on the mode of operation, and to provide efficient delivery of ions into the quadrupole mass filter. The ion lens operates at large negative voltages, with the last element before the quadrupole set at -200 V. Ions leaving the ionizing chamber (Fig. 6) are swept rapidly into the quadrupole entrance and decelerate to an average energy of 10 eV within 0.5 cm. This is an unconventional method of injection into quadrupoles, but appears to give good transmission of ions with energies down to 3 eV. The instrumental response to streaming ions on the low-energy tail is thus flatter than in conventional systems, which inject at 10-15 V.

Source parts in the ionization region are gold-plated. This feature insures the stability of electric fields in the low-energy drift space before the ion lens. Gold surfaces on these parts are also required to implement the O and O_2 separation scheme of Kayser and Potter.[5] Thus, UACS affords another chance to try a technique that was unique to the Open-Source Mass Spectrometer on Atmosphere Explorer-D (AE-D).[5]

Operation

The 32 UACS command states provide for both low-spatial-resolution scan modes, which are used for diagnostics or special studies, and a variety of high-spatial-resolution stepping modes, the modes most expedient for routine data collection. Figure 7 is an example of data collected in orbit at approximately 215 km altitude using the normal (non-RPA) mass scan. The scan proceeds in 0.25 mass unit steps, 10 steps per second, from mass 4 to mass 48, and then repeats. Peaks at masses 28, 32, 40, 44, and 46 are respectively N_2^+, O_2^+, Ar^+, CO_2^+, and NO_2^+. Peaks at masses 14 and 16 result not

only from singly ionized ambient N and O, but also from fractionated N_2 and O_2 and doubly ionized N_2 and O_2. The mass 32 peak results mostly from recombined atomic oxygen. Masses 30 (NO) and 46 are produced by recombination of N with O in the source. Masses 18 (H_2O) and 44 originate from source impurities.

The figure shows data taken on both the electrometer (lower panel) and SID (upper panel) and is an illustration of the large dynamic range obtainable with the dual-detector combination. At slightly higher gas densities, the deflector control circuit, which monitors the electrometer signal, would disable the SID deflector on scan steps near masses 28 (N_2) and 32 (O_2), so that only electrometer output would be available for the next decade increase in signal. For the combined detectors, a dynamic range of a million is realized and available at each new step in the mass program.

Figure 8 is an example of a scan using the retarding potential gate. In this case only, the retarding grid is set +2 V with respect to the drift space potential (see Fig. 6), and the drift space potential is varied with mass so that streaming ions of the selected mass exit the source with an average 10 eV total energy. It will be noted in Fig. 8 that most of the peaks seen in Fig. 7 have been suppressed. The remaining peaks correspond to ambient gases, O_2, N_2, and O. The mass 14 peak is attributed to ionization products of both N_2 and ambient N. Intensity in this mode is lower, corresponding to the small component of streaming gas, compared to the density of thermalized gas in the ion source.

Figure 9 is an example of a typical retarding mode operation for energy analysis. Here, mass is fixed at 28 (N_2) and the retarding grid is swept in 40 steps over the range from +5 to +15 V relative to the drift space. At the start of the sweep (step A) and at its mid-point (B), the retarding grid is driven to 0 V bias for one step to allow a normal mode determination of composition. Composition is therefore obtained at 20 km intervals along the track, concurrently with energy analysis.

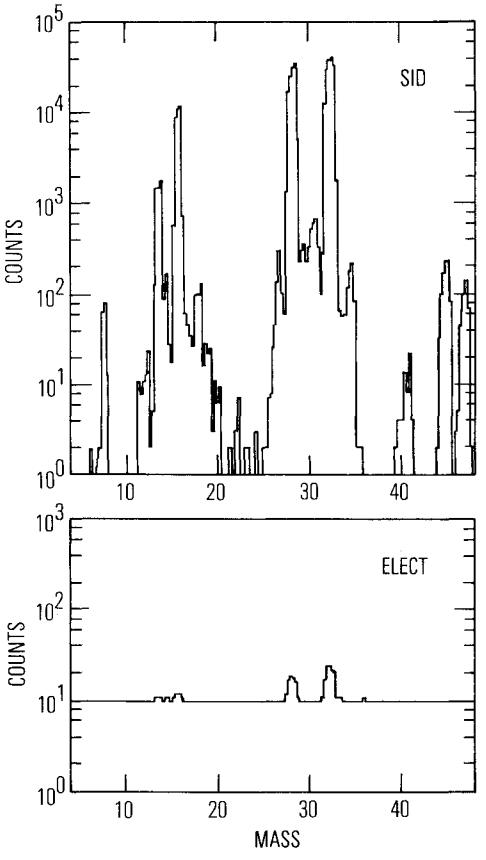

Fig. 7 Normal mode mass scan on SID and electrometer.

Ideally, the signal should drop to near zero above step 45 as the retarding potential cuts off the high energy tail of the distribution. As shown here, this does not happen: In fact, a slight rise in signal is seen. During calibration, a similar tail effect was noted even though the gas sample was static and no signal was obtained at lower step numbers. Thus, the tail appears to be related to reaction kinetics in the thermalized gas component, possibly in combination with focusing characteristics of the lens system. Steps C and beyond and steps before A are not used for measurement.

Other retarding mode programs are available. In one, for instance, the basic cycle shown in Fig. 9 is repeated at masses 16, 28, and 32 in succession, giving an energy analysis of O, N_2, and O_2. In another, the basic cycle ends with normal mode measurements at five selected mass numbers, allowing complete composition to be measured every five seconds along with the energy distribution of molecular nitrogen.

Calibration

Static calibration of the UACS is performed on a conventional calibration system similiar to that of Ref. 3. The method involves the recording of instrument detector output as a function of the ion source pressure over the anticipated range of inflight density. A number of sample gases are in-

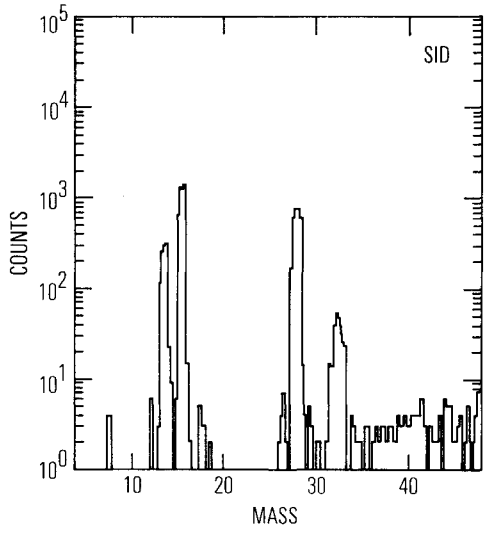

Fig. 8 Retarding (or flythrough) mode scan on SID.

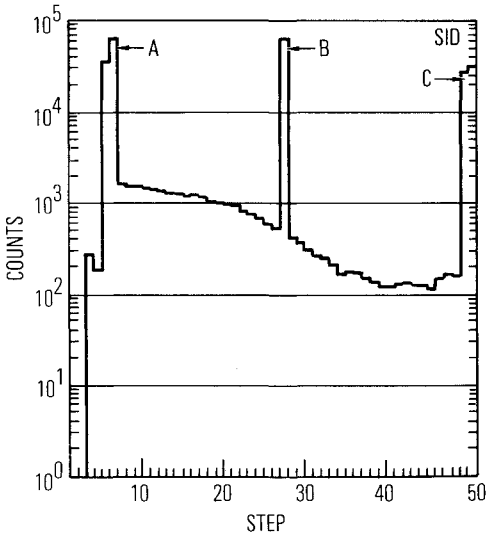

Fig. 9 Retarding mode energy analysis of N_2.

troduced into the calibration system, individually and in combination, to provide data on instrument response to most important thermospheric species. Atomic oxygen calibration is not yet practical in a static system, necessitating a cross-calibration in flight against the molecular oxygen signal. Experience has shown that cross-calibration is an effective alternative.[4,5]

Preliminary Flight Results

Examples of flight data were shown in previous sections. The mission returned measurements sufficent to allow an evaluation of the instrument concept. It is already apparent that the basic technique of retarding potential energy analysis can be applied successfully to neutral mass analyzers. Further study should indicate ways of optimizing the design for this purpose. Besides its immediate application to aeronomic data gathering, UACS could be a starting point for a diagnostic sensor to monitor space-borne neutral-beam experiments.

Summary

We have described a neutral mass analyzer package that is capable of providing both thermospheric composition data and retarding potential energy analysis of the incident neutral gas, leading to measurement of temperature and one component of the neutral wind. In addition to the energy analysis feature, it was demonstrated that a dual-detector system as described satisfies the requirement of thermospheric measurements for a large dynamic range.

Acknowledgments

This work was supported by the U.S. Air Force Systems Command's Space Division under Contract No. F04701-84-C-0085. The authors would like to thank former and present directors of the Space Sciences Laboratory, G. A. Paulikas and H. R. Rugge, respectively, and Atmospheric Sciences Department head J. M. Straus for their continued support of this research. Members of the Aerospace Space Test Directorate—Planning and Operations Department provided invaluable assistance in the areas of mission planning and experiment integration. Expertise in the installation and use of the vacuum-cap cutter mechanism was furnished by D. McIntyre of the University of Minnesota Physics Machine Shops.

References

[1]Hedin, A. E., "A Revised Thermospheric Model Based on Mass Spectrometer and Incoherent Scatter Data: MSIS-83," *Journal of Geophysical Research,* Vol. 88, Dec. 1983, pp. 10170-10188.

[2]Peltz, D. T., Reber, C. A., Hedin, A. E., and Carignan, G. R., "A Neutral-Atmosphere Composition Experiment for the Atmosphere Explorer-C, -D, and -E," *Radio Science,* Vol. 8, April 1973, pp. 277-285.

[3]Nier, A. O., Potter, W. E., Hickman, D. R., and Mauersberger, K., "The Open-Source Neutral-Mass Spectrometer on Atmosphere Explorer-C, -D, and -E," *Radio Science,* Vol. 8, April 1973, pp. 271-276.

[4]Nier, A. O., Potter, W. E., Kayser, D. C., and Finstad, R. G., "The Measurement of Chemically Reactive Atmospheric Constituents by Mass Spectrometers Carried on High-Speed Spacecraft," *Geophysical Research Letters,* Vol. 1, Sept. 1974, pp. 197-200.

[5]Kayser, D. C. and Potter, W. E., "A Technique for Mass Spectrometer Measurements of Atomic and Molecular Oxygen in the Lower Thermosphere," *Journal of Geophysical Research,* Vol. 83, March 1978, pp. 1147-1153.

[6]Philbrick, C. R., Narcisi, R. S., Baker, D. W., Trzcinski, E., and Gardner, M. E., "Satellite Measurements of Neutral Composition with a Velocity Mass Spectrometer," *Space Research,* Vol. 13, 1973, pp. 321-325.

[7]Spencer, N. W., Niemann, H. B., and Carignan, G. R., "The Neutral-Atmosphere Temperature Instrument," *Radio Science,* Vol. 8, April 1973, pp. 287-296.

[8]Spencer, N. W., Wharton, L. E., Nieman, H. B., Hedin, A. E., Carignan, G. R., and Maurer, J. C., "The Dynamics Explorer Wind and Temperature Spectrometer," *Space Science Instrumentation,* Vol. 5, 1981, pp. 417-427.

[9]Hedin, A. E., Avery, C. P., and Tschetter, C. D., "An Analysis of Spin Modulation Effects on Data Obtained with a Rocket-Borne Mass Spectrometer," *Journal of Geophysical Research,* Vol. 69, Nov. 1964, pp. 4637-4648.

[10]Kayser, D. C. and Potter, W. E., "Molecular Oxygen Measurements at 200 km from AE-D near Winter Solstice," *Geophysical Research Letters,* Vol. 3, Aug. 1976, pp. 455-458.

[11]Knutson, J. R., Kayser, D. C., and Potter, W. E., "Mass Spectrometric Measurement of Thermospheric Wind," *Journal of Geophysical Research,* Vol. 82, Nov. 1977, pp. 5253-5256.